INSTYUT BADAN JADROWYCH

Report "P" No. 823/XVIII/PP, Warsaw 1967

(Submitted to "Przegladzie Elektrotechnicznym")

SWITCHING OF HIGH CURRENT IMPULSE GENERATORS WITH FOUR ELECTRODE SPARK GAPS

by

A. Jerzykiewicz and M. Sadowski

Translated at CERN by T.H. Hofmokl and L.M. Celnikier

(Original : Polish)

(CERN Trans. 68-4)

Geneva

March, 1968

INTRODUCTION

The switching of circuits in the impulse current generators used to produce and maintain hot plasmas is done by means of controlled spark gaps (1). Several typical functions of spark gaps can be defined :

a) the simultaneous connection of parallel generator units to one terminal
b) the time ordered connection of several generators to one terminal
c) the simultaneous or time ordered connection of several generators to several terminals at one experiment
d) the short-circuiting of a terminal, which would usually take place at the moment of maximum current

Each separate case places different technical restrictions on the spark gap and on its triggering circuit.

The behaviour of a spark gap is characterized by the following parameters : the jitter time $\Delta\tau_z$ as a function of the steering coefficient, the limit steering coefficient, and, for most spark gaps, the length of the triggering pulse ti. It is assumed that the time distribution of triggering of all spark gaps serving a specified function is

$$\Delta\tau_z = \tau_{z\,max} - \tau_{z\,min}$$

where $\tau_{z\,max}$ and $\tau_{z\,min}$ are the maximum and minimum times to trigger the spark gaps.

The steering coefficient of a spark gap is $K_s = \frac{Ups}{U}$ where

Ups is the static break down voltage of the spark gap

U the loading voltage of the capacitor in the circuit containing the spark gap.

The limit steering coefficient is equal to $Ksg = \frac{Ups}{Upmin}$ where Upmin is the minimum breakdown voltage of the spark gap at triggering.

When the first spark gap has been fired, a voltage wave of amplitude U_1 reaches the remaining spark gaps after a time $t_\ell = \frac{2\ell}{v}$ where l is the length of the connection between each spark gap and terminal, and v is the velocity of the wave.

If the remaining spark gaps had not fired, while the voltage difference between each of the two electrodes had been U - 0 (U being the

loading voltage of the bank), then after a time t_l this difference would be $U - U_1$. After removal of the wave resistance of the connection, the difference $U - U_1$ is initially small, changing with time in a way determined by the circuit parameters of the circuit in which the spark gap is placed.

Two areas of spark gap operation should be discussed. If $\Delta\tau_z < t_l$ and $\Delta\tau_z \ll \frac{T}{4}$ (T being the resonant period of the discharge circuit), and if the lifetime of the triggering impulse is suitably chosen, then all spark gaps will fire if only the loading voltage of all circuits be in the region : $Upmin < U < Ups$.
Under these conditions the limit steering coefficient should be chosen according to : the voltage range of the generator, the ageing of the spark gaps, and the required reliability. This coefficient could approach unity for generators built for one voltage.

If $\Delta\tau_z > t_l$ and the triggering pulse lives sufficiently long, then firing can occur only when

$$\frac{Ups}{U-U_1} < Ksg \qquad (1)$$

$U - U_1$ is small. Therefore, in order that $\Delta\tau_z \ll \frac{T}{4}$, it is necessary that the limiting steering coefficient be large. Spark gaps having a small limiting steering coefficient can fire when inequality (1) is satisfied, if the triggering pulse is long enough or if there are secondary triggering contributions. Spontaneous breakdown can take place after a time greater than $\frac{T}{4}$ because $U - U_1$ could exceed the static firing voltage. This type of operation is associated with a local overload, which is dangerous to the insulator, while at the same time the steepness of the resulting current and its amplitude are less than expected.

In case (b) the switching on of the second and eventually the following generators happens when the terminal is under voltage. Therefore in such generators it is usual to use spark gaps with large steering coefficients and $\Delta\tau_z$ must be much less than $\frac{T}{4}$.

In case (c) (the switching on of generators to different terminals), the acceptable firing distribution is defined by the experimental requirements, and these are usually less stringent than in the other cases.

In case (d), the spark gaps which short circuit do so most often at the moment of the first maximum current, and therefore when the voltage across them is near to zero. Thus, they must have large steering coefficients and $\Delta\tilde{\tau}_z \ll \frac{T}{4}$.

Therefore, in general, the time distribution of firing should in all cases be much less than $\frac{T}{4}$, while for spark gaps having small limiting steering coefficients, the additional inequality

$$\Delta\tilde{\tau}_z < \frac{2l}{v}$$

must be satisfied.

Assuming that $\Delta\tilde{\tau}_z$ be sufficiently small when $\Delta\tilde{\tau}_z < 0{,}1\ \frac{T}{4}$, and taking into account that the frequency of large generators is in the region of 10 - 100 kHz, the limiting values are :

$\Delta\tilde{\tau} < 2{,}5\ \mu s$ for 10 kHz
$\Delta\tilde{\tau} < 0{,}25\ \mu s$ for 100 kHz

The distance separating spark gaps from terminals is usually 2 - 15 m. Assuming a wave velocity of 300 m/μs for tape connections and 150 m/μs for cable connections, we can derive for $\Delta\tilde{\tau}_z$ the intervals

13 - 100 ns for tape connections
26 - 200 ns for cable connections

It can be seen from the above, that the restrictions on the majority of spark gaps having small limiting steering coefficients are more rigorous.

The problem of the interaction of four electrode air spark gaps and vacuum spark gaps was investigated in the Institute of Nuclear Research. The first part of the results concerning air spark gaps is presented in this paper.

Four electrode air spark gaps (2,3) shown in figure 1 were investigated. This type was chosen for its properties, and in particular because of its effective independance from polarity, and because of the possibility of obtaining a value of the steering coefficient greater than 2, which cannot be done with trigatrons.

The characteristics of such a spark gap depend on its own parameters and those of the circuit in which it is placed. The former are : the interelectrode capacity, the relation of the static firing voltage of the

first gap to that of the second, the static firing voltage across the gap between the (bias) electrode and the central one, and the self-induction of the spark gap. The latter are : steepness and amplitude of the triggering voltage and its lifetime, induction of the connections with the circuit, wave resistance of the circuit, the terminal parameters, relation between the resistances of the voltage dividers, and the value of the capacitor which is sometimes connected in parallel to the central electrode and earth or in series between the (bias) electrode and the triggering circuit.

The idealized representation of the voltage on the (bias) electrode during firing is shown in figure 2. Diagram(a) considers the case of small steering coefficients, when breakdown has taken place initially in the gap having the larger static firing voltage, while the breakdown in the next gap is a consequence of the overload produced by a polarity change of the capacitor across this gap. The largest value of the steering coefficient for which such a mechanism is still possible is equal to the value of the coefficient for which the probability of breakdown of each gap is the same, and could be estimated arithmetically.

The equations for this case are :

$$U - U_1 + Ui = KuUp_2$$

$$Ui - U_1 = KuUp_1$$

where U_1 the voltage of the central electrode

Ui triggering voltage

Ku impulse coefficient

Up_1 and Up_2 static breakdown voltage of the gap.

The impulse coefficient in the steepness range applied in the experiment, varied between the limits 1,2 and 1,3. For the purposes of calculation, Ku was taken to be 1,25. Taking into account that the steering coefficient $Ks = \frac{Ups}{U}$ and that the relation of the firing voltages of both gaps and the voltage dividers $Kp = \frac{Up2}{Up_1}$, the equations can be rewritten in the form

$$\frac{UpsKp}{Ks(kp+1)} + Ui = 1,25\ \frac{UpsKp}{Kp+1}$$

$$Ui - \frac{Ups}{Ks(kp+1)} = 1,25\ \frac{Ups}{Kp+1}$$

Eliminating Ui and simplifying, we obtain

$$K\overset{\downarrow}{s} = \frac{Kp+1}{1,25(Kp-1)} \qquad (2)$$

For the value Kp = 1,6 used in the investigations, the steering coefficient was calculated to be 3,45.

The condition that firing occurs in the second gap as a consequence of overloading is given by :

$$KoU = Up_2$$

where Ko is the coefficient of overloading, and Ku $\tilde{=}$ 1 because of the relatively slow variations in the limit case. After re-arrangement, we can obtain the maximum value of the steering coefficient

$$Ksm = Ko(Kp + 1) \qquad (3)$$

We obtain the optimal value of Kpo and Kso as functions of the overloading coefficient by comparing (2) and (3)

$$Kpo = \frac{1+1,25Ko}{1,25Ko}$$

$$Kso = 2Ko + 0,8 \qquad (4)$$

It follows from the formulae that the larger the overload coefficient the larger the steering coefficient, and Kp tends to 1.

In our investigatons, Kp was 1,6.

The measured values of Ksm were 2,5 $\div$ 2,7 in all circuits. By substituting these values in formula 3 we obtain Ko$\approx$1.

One way to increase the limiting steering coefficient of 4 electrode spark gaps is to increase the overload coefficient by connecting a capacitor of several pF between the central electrode and earth. In this way, Fitch (2) obtained a steering coefficient of 6,8 for Kp = 1, which corresponds to the overload coefficient being 3,4 according to formula (3). An increase of the interelectrode capacitance decreases the steepness of the triggering pulse. This is inconvenient, if a steering coefficient greater than is given by formula 3 is required.

We must now examine the behaviour of spark gaps when steering coefficients are greater than Ksm. Two cases can be distinguished : firstly

when Ksm = $K\dot{s}$ = Kso and secondly when Ksm is smaller than $K\dot{s}$. In the first case, it is more probable that the first breakdown will take place in the gap having the smaller static firing voltage. This is true for all steering coefficients. In the second case, it is more probable that breakdown will take place in the gap having larger static firing voltage while the overload coefficient Ko is too small to initiate breakdown in the second gap. This is valid for values of the steering coefficient in the range Ksm $\div$ $K\dot{s}$. When Ks $>$ $K\dot{s}$, it is more probable that the first breakdown will take place in the gap having the lower static firing voltage. In both cases, the breakdown across the second gap can take place only when the voltage generated by the triggering pulse across the inductor on the short circuiting gap exceeds the static firing voltage of the second gap. The idealized representation of the voltage across the (bias) electrode during operation as described above for is shown in figure 2b. In order to increase the voltage across the inductor during the growth of the discharge, the spark gap is sometimes connected to the circuit by means of a coil having a suitable ferrite core (4) so that the coil's inductance is large during the growth of the discharge and falls for the current of the main discharge. To eliminate discontinuities when operating in this mode, and for Ksm $\div$ $K\dot{s}$ the coefficient Kp should be matched to Ko using formula (4).

An analysis presented farther on demonstrates that, apart from the case discussed above, the discharge grows simultaneously in both gaps when the triggering pulse has a high steepness, and the steering coefficient is larger than Ksm.

TRIGGERING CIRCUITS

It follows from figure 2 that the steepness of growth of the triggering voltage has a direct influence on the interval before firing, and an indirect influence on the time distribution during this interval.

The circuits producing steep voltage pulses can be grouped into 3 basic types.

In the first type (figure 3a) the pulse is produced by the operation of a pulse transformer powered by a condenser bank discharging through the primary winding of the transformer by means of a thyratron. The pulse

steepness depends on the resonant frequency :

$$f = \frac{1}{2\pi\sqrt{LC}}$$

where L is the inductance and C the capacity of the primary circuit. The load on the secondary of the transformer is capacitative, and is relatively large because of the arrangement of the cables and connections between the spark gaps. This capacity determines the quantity of energy which the transformer must transmit, and indirectly determines the energy stored in the primary circuit. In order to achieve a high steepness of the voltage, it is necessary to decrease the primary inductance, the smallest value being 200 - 300 nH, and to decrease the capacity, which under constant energy conditions requires an increased loading voltage. There is little sense in using transformers in this way, and it is much better to use circuits in which the voltage is applied directly to the triggering cables.

The suggested (5) arrangement of parallel transformers is complicated and uneconomical.

The second type (figure 3b) consists of a low inductance capacitor, which is discharged through a secondary spark gap on a parallel cable.

The pulse entering the cable is expressed by :

$$U = U_{\tau}\left(1 - e^{-\frac{tZ}{nL}}\right)$$

where U_{τ} the loading voltage of the capacitor

Z the wave resistance of the triggering cable

n the number of cables

L inductance of the secondary spark gap, the connections and the condenser.

The instantaneous steepness is expressed by :

$$\frac{dU}{dt} = \frac{U_{\tau}Z}{nL}\, e^{-\frac{tZ}{nL}}$$

and is directly proportional to the loading voltage and cable wave resistance, and is inversely proportional to the number of cables and the inductance of the connections. The steepness depends also on the time of growth of the discharge in the secondary spark gap.

This system was successfully used to trigger trigatrons (6) and vacuum spark gaps because it is possible to force out high currents. There are certain disadvantages in applications to 4 electrode spark gaps. If the triggering cables are connected directly to the (bias) electrode, then the variation of voltage across the secondary spark gap is a function of the main bank loading voltage for constant secondary capacitor loading voltage. The secondary capacitor must be insulated from earth in order to inhibit the closing of the triggering circuit by earth. A galvanised connection through the cables of all (bias) electrodes produces an overload when one of the spark gaps does not work (figure 4)

In general, the disadvantage of this system is the dependence of the pulse steepness on the number of cables in parallel (figure 5).

Such a system is justified only when the magnitude of the triggering current influences the operation of the spark gap. Such a dependence has not been observed for the spark gap investigated.

Figure 3c shows a pulse circuit based on the principle of a loaded cable line short-circuited through a spark gap and a circuit with inductance L. A pulse of instantaneous steepness

$$\frac{dU}{dt} = \frac{UZ}{L} e^{-\frac{tZ}{L}}$$

is produced.
The advantage of such a system is an independence from the number of cables and from the pulse steepness.

A capacitor of small capacitance connected in parallel with the spark gap is sometimes used. Neither the steepness of a pulse nor the characteristics of the tested spark gap were affected by the connection of a 1250 pF condenser.

An oscillatory discharge develops in the circuit - secondary spark gap, triggering cable, chopping condenser, parallel connected main condenser and terminal - after the passage of the triggering pulse and the firing of the tested spark gap. Therefore, high frequency oscillations, whose amplitude depends on the distribution of induction in the above circuit, must be added to the voltage across the terminal. These oscillations can be

damped by the inclusion of active resistances in series. The amplitude and the triggering pulse steepness are decreased as a consequence (figure 5). We may expect that applying in this way a resistance having non-linear characteristics should slightly reduce the pulse amplitude and increase its steepness. This follows because as the voltage wave reaching the non-linear resistance increases, so increases the ratio of the transmitted amplitude to that of the reflected one. Experiments carried out with a resistance of about 100Ω at 5 kV and one of 1,8Ω at 20 kV confirmed the above predictions (figure 5). The U pulse steepness was about 2,3 times larger than in the case when a 100Ω linear resistance was used, and 1,35 times larger than in the case when no damping resistor was used.

The growth steepnesses which were obtained never exceeded 1,4 kV/ns, because of the relatively large inductances in the circuit. We did not reduce them, because our tests were of a phenomenological character, while an increased steepness would have required the use of voltage dividers with a very short response time for the measurement of voltage. This would have complicated the measuring technique. The input inductances of the cables used in cases 3b and 3c were nearly equal. System's 3b more favourable pulse steepness follows from the use in 3c of the chopping condenser. This was associated with an increased inductance on the part of the tested spark gap.

Below are tabulated the results of the tests carried out on the various systems.

System as in figure	Number of parallel circuits	Number of users	Steepness of triggering pulse KV/ns	Oscilloscope display of pulse as in figure
3A	6	6	0,029	6a
3B	6	$\frac{6}{1}$	according to fig 5	6b
3B	1	1	according to fig 5	6c
3C	1	1	according to fig 5	6d and 6e

The pulse steepness is defined as the tangent of the angle between the straight line passing through 0,3 Up and 0,9 Up and the time axis (Up - the smallest breakdown voltage). The voltage was measured on the (bias) electrode when the main bank was discharged.

TESTING METHODS

It is relatively easy to measure the time interval distribution up to firing. To do this, we usually use an oscillogram, analysing either the voltage signal coming directly from the circuit in which the spark gap is placed (7), or the signal $\frac{di}{dt}$ from the Rogowski belt (8).

Several curves may be recorded on one frame of film, from which τ and $\Delta\tau$ can be immediately deduced. Only incomplete conclusions may be drawn about spark gaps in the parallel configuration from the characteristic $\Delta\tau = f(U)$ or $\Delta\tau = f(Ks)$. The characteristics prepared in this way do not include the influence of individual differences between spark gaps and connections. In order to obtain from measurements on one spark gap the full information concerning the usefulness of spark gaps working in the parallel configuration, it would be necessary to test several spark gaps. The characteristic $\Delta\tau z = f(Ks)$ obtained in this way leads to final conclusions about the interactionof spark gaps in the parallel configuration when the circuit parameters of the generator are the same as in the test circuit. Consequently, it is much better to test the interaction of spark gaps in the parallel configuration. Such tests are technically more difficult to carry out, because it is necessary to compare simultaneously several processes to obtain the arithmetical values of the firing distribution. Several multi-chanel oscillographs or high-speed cameras are used to do this (9).

In the latter case (special)photographs of the spark gap discharge are taken, using either optical fibres (to observe the optical phenomena within the spark gap) or secondary spark gaps connected in parallel with the tested spark gaps.
A qualitative assessment of the interaction of parallel configurations can be obtained from a comparison of the oscillogram of total current with that of the currents in the parallel branches.

REDUCTION OF THE SPARK GAP CHARACTERISTIC

The basic spark gap characteristics were measured in the circuits drawn in figure 7a and 7b using the oscillograph Ok-19M. Ten oscillogram passes were taken for each point. An example of such an oscillogram is shown in figure 8. The time to breakdon was defined to be the arithmetic mean of the longest and shortest time, counting from the initiating pulse to the moment of firing of the second spark gap. The time distribution to breakdown was calculated as the difference between the longest and shortest time to fire. All measurements were done on the spark gap in which the static voltage was 27,5 kV, the static voltage across the gap on the condenser side was 17 kV and the static voltage on the earth side was 10,5 kV. The ratio on the voltage divider across the gaps was equal to the ratio of their static firing voltages, and was equal to 1,6.
The characteristics $\tau_{iz}\tau = f(U)$ for several values of loading voltage, in the initiating circuit drawn in figure 7a, are shown in figure 9.

In both sets of characteristics, there is an interval in which the time distribution to firing is large. This interval lies between values of the steering coefficient 2,6 $\div$ 3,5 and agrees with the value previously calculated for the Ksm and Ks intervals. The discontinuity of the characteristics corresponds to Ks = 3,5 and the times to fire vary from 230 ns to infinity. According to formula 2, for Ks $\cong$ 3,5, it is equally probable that breakdown occurs in the first or second gap. This, together with the different parameters of the circuits connected in series with each gap, produces such significant fluctuations. The discontinuity disappears when the loading voltage of the initiating circuit is about 50 kV, but the time distribution to fire remains above 200 ns.

An increase of the loading voltage of the initiating circuit for values of the steering coefficients in the range 1 to 2,6 does not affect the time distribution to fire, but does reduce the growth time of the discharge. This is shown in figure 10.

When the steering coefficient is greater than 3,5, a voltage increase on the initiating circuit shortens the time to firing and increases the time distribution. The characteristics $\Delta\tau = f(Ui)$ reaches its minimum value at Ui $\cong$ 25 kV.

When the steering coefficient is between 2,6 and 3,5 firing in both gaps is often observed. The discharge in the main condenser develops significantly later. This is a consequence of the compensation of the voltage on the main condenser by the initiating voltage.

Thus, a shorter pulse time leads to a shorter time to fire.

This was tested for two cable lengths and with a damping resistory connected in series with the cable. This is shown in figure 7b. For the first cable length, the pulse time was 210 ns, and for the second one was 110 ns. The characteristics obtained are prsented in figure 11. In this configuration the time to fire for values of the steering coefficient greater than 2,6 was shorter, and in the whole range of operation does not exceed the lifetime of the initiating pulse. The fluctuations in the time to fire were also reduced. An analysis of the oscillograms also shows that if the steering coefficient is larger than 2,6 for times to fire less than 100 ns, then the discharge develops simultaneously in both gaps.

When the steering coefficient is less than 2,6 the fluctuations in the time to fire are increased, particularly when the pulse has a small steepness (Ui = 20 kV, linear damping resistor figure 11). The reasons for this are the significant differences in the original steepness of the initiating pulses, caused by the development of the discharge in the secondary spark gap. In connection with this, the distribution of times to breakdown of the first gap in the tested spark gap was equal to 40 ns. For greater steepness, this distribution was smaller and did not exceed 10 ns.

It is to be expected that when an additional spark gap creates the leading edge of the initiating pulse, and is placed between the initiating cable and the tested spark gap, the fluctuations in the time to fire would be reduced.

In order to obtain small fluctuations in the time to fire in the configuration 7b, it is necessary to initiate breakdown by a pulse having steepness larger than 0,6 kV/ns. When this condition is imposed, then increasing the cable loading voltage to above 20 kV has little influence on the time to firing and on its fluctuations. On the other hand, the steering coefficient grows even to above 30. An apparent inconsistency between the

necessary requirements derived from the measurements in configuration 7a and 7b and those concerning pulse steepness appeared at this point. This inconsistency follows from the method used to measure steepness in configuration 7a when the main bank is not loaded. While the characteristics were being measured, the potential difference across the secondary spark gap was higher and equal to the sum of the loading voltage of the secondary condenser and the voltage of the central electrode in the tested spark gap. The steepness of the initiating pulse was greater than figure 5 would indicate, and moreover, was different for each point of the curves

$$\tau_i \text{ and } \Delta\tau = f(U)$$

It can be seen from figure 9 that the influence of polarity on spark gap operation is negligible.

The static firing voltage across the (bias) and central electrodes has a small influence on the characteristic $\tau_i \Delta\tau$. Measurements done at 0,3 and 2,9 kV showed no difference within the measurement accuracy. The times to fire and their fluctuation were increased by short circuiting the (bias) and central electrodes.

TESTS ON THE INTERACTION OF PARALLEL SPARK GAPS

The circuit shown in figure 12 was built in order to test the results obtained for one spark gap. This circuit consisted of 6 parallel branches. The static firing voltage was 33 kV. The ratio of the static firing voltages of both gaps and of the voltage divider was 1,6. In this configuration, we did not measure the characteristics. Instead, the lower limit of voltage for which the system worked correctly was defined, and two types of measurements were done. The first type using open switches, shown in figure 12, corresponds to the configuration of 6 parallel branches feeding independent terminals. A pulse transformer, connected to the (bias) electrodes in the spark gaps through 2500 pF condensers, initiated firing in this case. The voltage was measured using a 15,2 kΩ voltage divider connected between the high tension side of the pulse transformer (figure 3a) and the oscillograph OK-17-M. The times to fire of individual spark gaps at a pulse steepness of 0,029 kV/ns were in the range 0,6 - 0,85 μs for values of steering coefficient of 2,5 (which is the maximum value of the coefficient for which operation is certain).

Some additional tests about the fluctuations in operations were done optically. To do this, a secondary spark gap having a static firing voltage of about 2 kV was connected in series with each tested gap. The secondary spark gaps were placed close together in a vertical straight line. A high speed soviet camera, type SFR-2M, was used. This camera has a rotating mirror, which projects the image into a stationary section of film. At the maximum rotating speed of the mirror (75000 turns/min.), the light beam moves at 3,75 mm/μs.

The object to be photographed was relatively large. It was therefore necessary to adapt the optical structure of the camera, by adding a suitable objective and collimating slit. An objective of type Jupiter 3 having f = 1 : 1,5 and focal length 5 cm was used when the camera was at a distance 5 m from the spark gaps. The collimating slit, whose width varied between 0 and 0,5 mm was placed at the focus of the objective. The other elements of the optical system were not changed.

The camera was set up in such a way, that only the images of the secondary spark gaps were registred. The collimating slit was used to select a narrow band covering 6 gaps. Consequently, the 6 spots of light on the film corresponding to the firing of all spark gaps, become 6 bands. The relative displacement of the leading edges of the bands correspond to the fluctuation of times to fire of the gaps.

The effective length of film was limited to 37,5 cm, while at the same time the recording speed of the light beam was very high. It was therefore important to synchronise the processes exactly. To do this, the system governing the firing of the spark gaps was triggered by a pulse coming from the camera control system when the mirror was suitably positioned. Figure 13a shows a typical photograph taken when Ks = 2,5 using a pulse transformer. The fluctuation of the firing times, measured by the optical method, was 0,25 μs. Figure 13b shows, for comparison, a photograph taken for the configuration drawn in figure 12 (open switches). The initiating pulse was produced by the secondary configuration shown in figure 3b (Ui = 30 kV, Ks = 2,1). In this case, the distribution of times to firing is smaller than 50 ns, the measurement errors being $\pm$ 10 ns.

A system consisting of 6 parallel branches feeding one terminal

is produced by closing the switches of figure 12. The initiating pulse in this case was produced by the configuration shown in 3b. The operation was checked by using the Rogowski belt and an oscillograph OK-17M. The variation of the total current was compared with the variation in one branch (figure 14). Simultaneously, the time to fire and its distribution was investigated for branches 1 and 5 using the voltage divider and an oscillograph OK-19M. 10 passes were registred on one photograph. This configuration worked correctly for steepness of the initiating pulse as drawn in figure 5 when the steering coefficient was 1 - 2,7. The time to fire was 195 ns for a value of the steering coefficient 2,65, for a 20 kV pulse, with a distribution of 64 ns ; it was 155 ns for a value of the steering coefficient 1,65, for a 20 kV pulse, with a distribution of 38 ns ; it was 140 ns for a 30 kV pulse with a distribution of 55 ns. In the latter case, while the distribution for one of the spark gaps was 10 ns and for the other was 15 ns, the times to fire differed by 38 ns. In the other cases the differences in the times to fire were smaller than 2 ns, while the differences in the distributions of times to fire were about 25 % of their nominal values. This confirms that the tests must include the effects of differences in spark gap construction and connection.

When the steering coefficient was larger than 2,7, our system did not work because the steepness of the initiating pulse was too small.

CONCLUSIONS

The best method of firing four electrode spark gaps is the one based on the principle of the short circuited loaded cable line. In order to damp oscillations in this configuration, it is useful to apply non-linear resistors, which increase steepness. When the steering coefficient is in the range $1 \div 3$ and for suitable pulse steepnesses, it is enough to load the line to a voltage of 75 % of the static firing voltage of the spark gap. For correct operation at higher steering coefficients, it is necessary to load the line to higher voltages. The lifetime of the pulse which initialises firing should be $1,2 - 2\tau_z$.

When four electrode spark gaps are connected in circuits feeding individual terminals, and when the restrictions on the time distribution of firing are not too severe, pulse transformers may be successfully applied in the range of values of the steering coefficient 1 - 2,5.

Four electrode spark gaps may be always used as connection elements in steep impulse current generators, whenever the parameters of the discharge initiating pulse, the time to fire and its distribution are suitably chosen.

REFERENCES

1- JERZYKIEWICZ A, NOWIKOWSKI J. : Application of Pulse Generators for High Temperature Plasma Research. Przegl. Elektr. 1967, vol. XVIII z.4 s.143

2- FITCH R.A., McCORMICK N.R. : The Modes of Operation of a Cascade Spark Gap for Precision Switching Proc. 4-th Intern. Conf. on Ionization Phenomena in Gases, Uppsala. August 1959 vol. 1 p. 463

3- TUCK J.L. : Review of Controlled Thermonuclear Research at Los Alamos for mid. 1958. Proc. 2-nd. U.N. Intern. Conf. Peaceful Uses of Atomic Energy. Geneva 1958, vol. 32.

4- KLEMENT G., KUNZE R.C., von MARK E., WEDLER H. : Ferrite Decupled Crowbar Sparkgap Proc. 4-th Symposium on Engineering Problems in Thermonuclear Research Frascati Rome May 1966

5- THEOPHANIS G.A. : Millimicrosecond triggering of high voltage spark gaps. Rev. Sci. Instr. 1960 Vol. 31 No 4 p. 427

6- HINTZ E., BEARWALD H. : The Three Electrode Spark Gap and its Application for the Simultaneous Switching of Many Parallel Spark Gaps. Proc. 4-th Intern. Conf. on Ionization Phenomena in Gases, Uppsala. August 1959. Vol. 1 p. 468.

7- GRUBER G., MULLER G. : Steep Voltage Triggering of a Simple Two Electrode Crowbar Gap. Proc. 4-th Symposium on Engineering Problems in Thermonuclear Research, Frascati-Rome, May 1966

8- HAGLSPERGER H., KLEMENT G., KUNZE R.C., MULLER G. : Combined Start and Crowbar Sparkgap with Wide Operating Range, ibidem.

9- OERTEL G.K., WILLIAMS M.D. : Optical Measurement of Switch Jitter. Rev. Sci. Instr. 1965. Vol. 36, No 5, p. 672

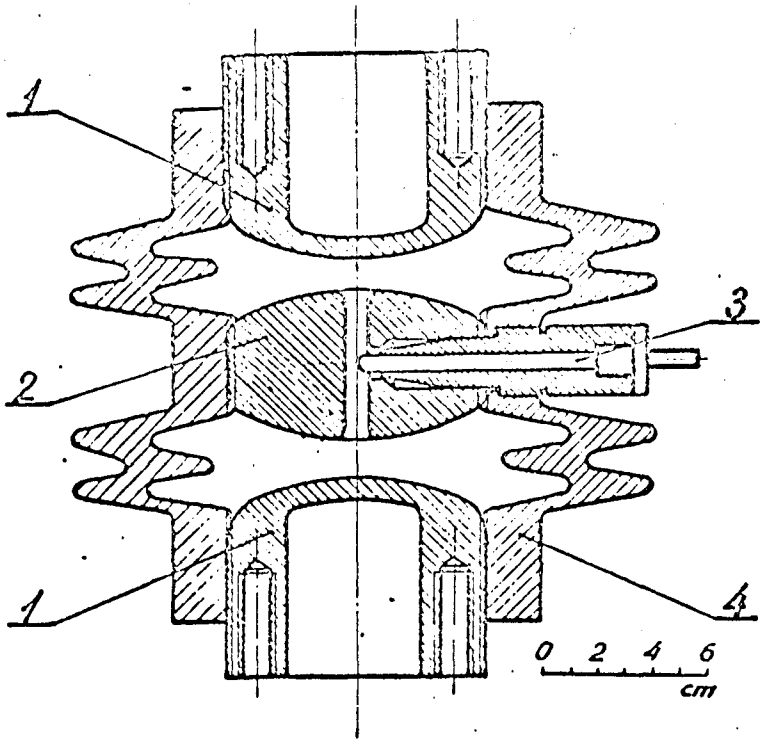

Figure 1 : The cross-section of a four electrode spark gap :

1- main electrodes

2- central electrode

3- bias electrode

4- insulator

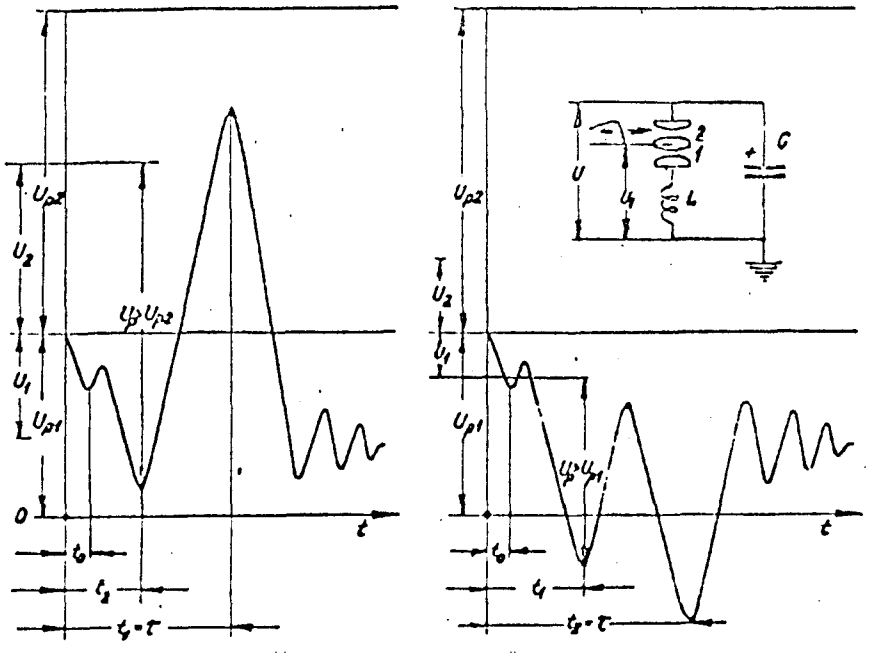

Figure 2 : An idealized sketch of the voltage on the (bias) electrode in the 4-electrode spark gap during firing :

a- for KsKsm

b- for KsKs'

Up_1, Up_2 are the static firing voltages across gaps 1 and 2

Up is the instantaneous voltage across the gap

t_o, t_1, t_2 are the times to fire of the secondary gap, and gaps 1 and 2 respectively.

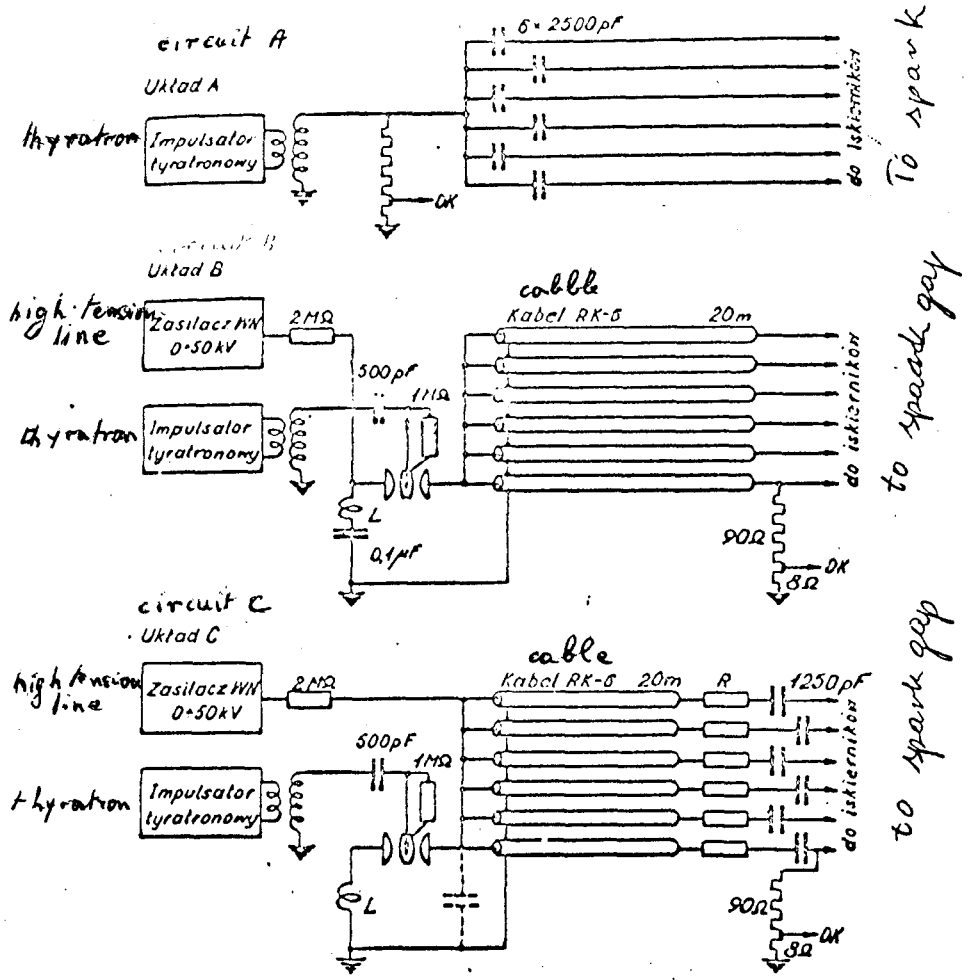

Figure 3 : Sketches of the circuits used to generate initiating pulses.

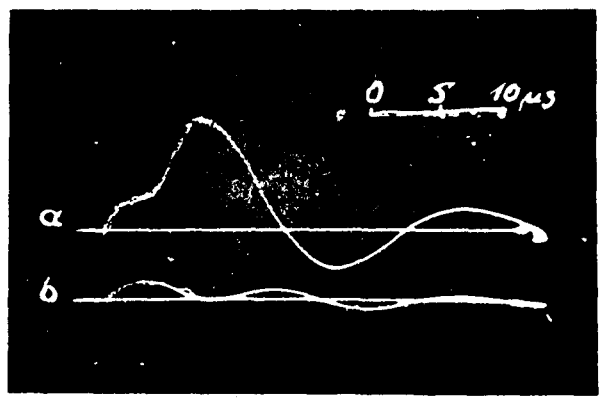

Figure 4 : An oscillogramm of the currents produced by the configuration shown in figure 12, when its operation was incorrect :

a- total current

b- current in section 1 (twice the frequency)

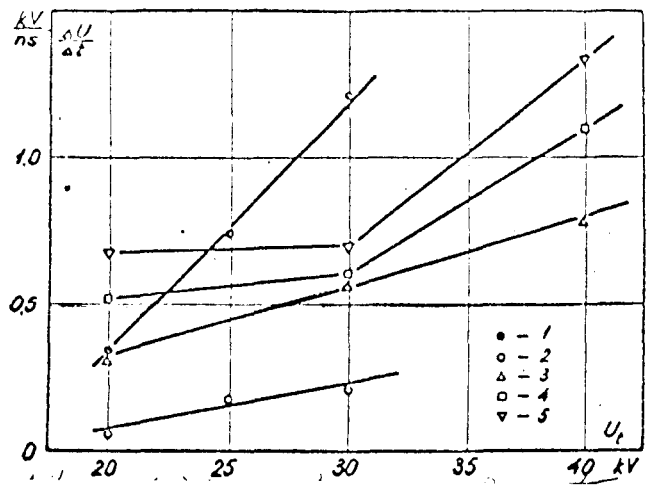

Figure 5 : Steepnesses of the initiating pulses as functions of the loading voltage of the bias electrode in configuration 3b

1- for 1 sparkgap

2- for 6 sparkgaps in configuration 3c

3- at R = 100

4- at R = 0

5- for non-linear - 1,8 at 20 kV and 100 at 5 kV/.

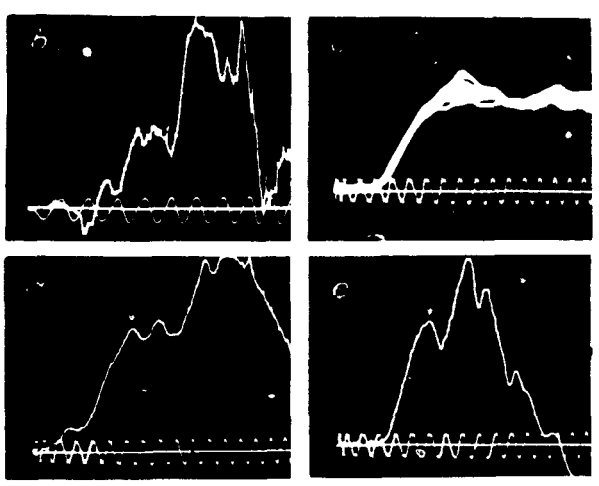

Figure 6 : Oscillograms of the voltage pulses on the (bias) electrode :

a- the 6 parallel branch circuit as in figure 3a (the lower line is the current in section number 1 and a 5 μs time signal)

b- the 6 parallel branch circuit as in 3b, scale 10 MHz

c- 1 branch, as in 3b, 10 passes, scale 100 MHz

d- 1 branch, as in 3c, R - linear, scale 100 MHz

e- 1 branch, as in 3c, R - nonlinear, scale 100 MHz

In the cases b and e the branches were loaded to 20 kV. The points marked with arrows - firing interval on the earth side.

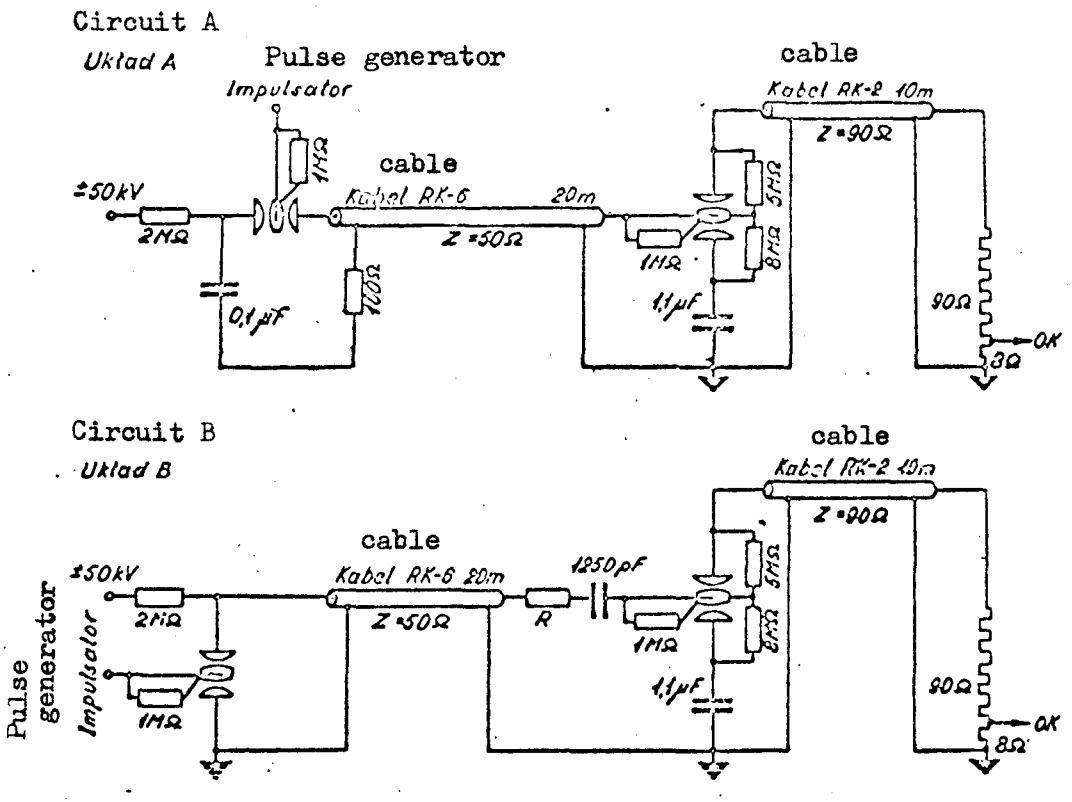

Figure 8 : Schematic representation of system used to measure spark gap characteristics.

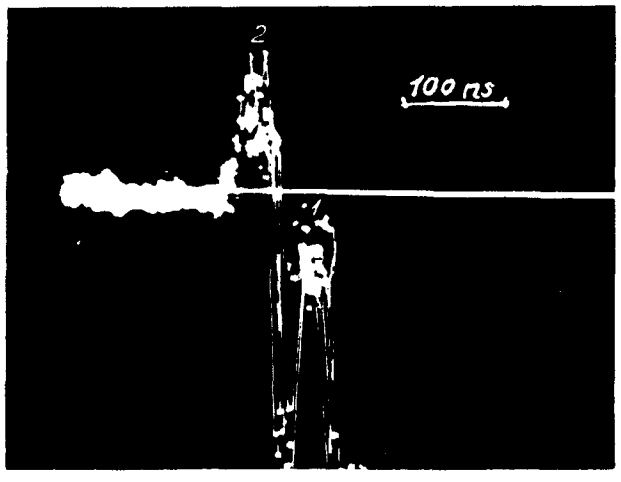

Figure 8 : A typical oscillogramm of 10 superimposed voltage curves. The loading voltage of the main electrode is 17,5 kV, and that of the bias electrode is 30 kV.
Point 2 represents firing on the condenser side.
Point 1 represents firing on earth side.

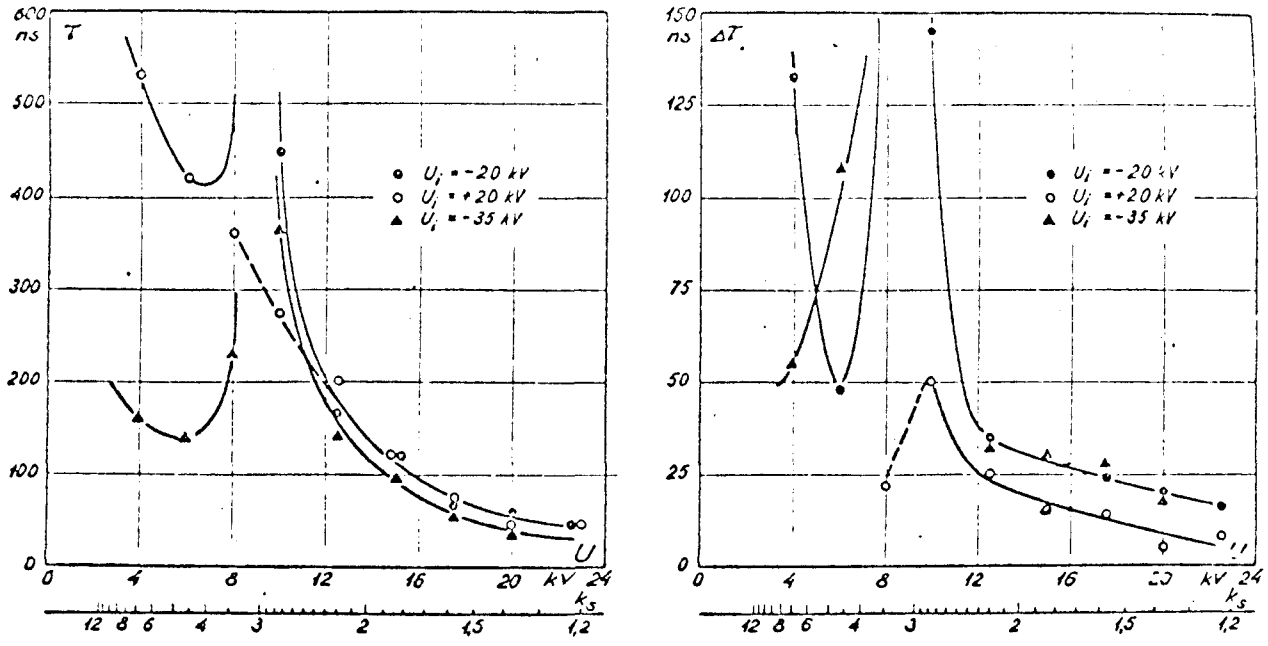

Figure 9 : Characteristics of times to fire and of fluctuations of times to fire as functions of the loading voltage of the main electrode for different loading voltages of the (bias) electrode. Figure 7a shows the system of measurement. The change of loading voltage on the main electrode is opposite to that in the initiating pulse.

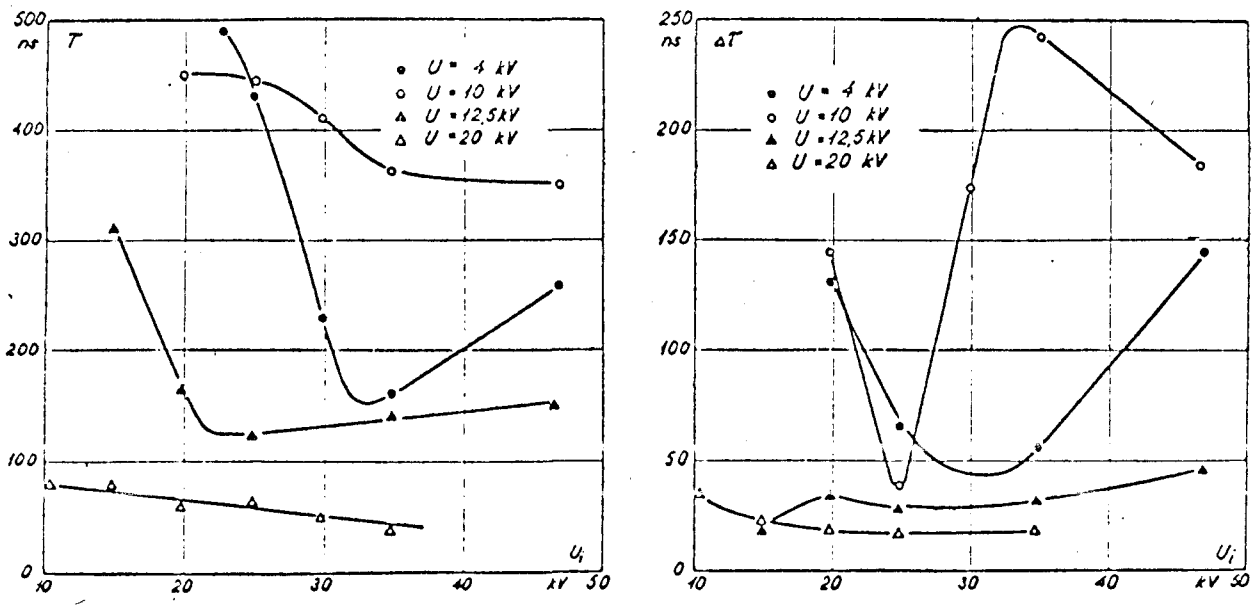

Figure 10 : Characteristics of times to fire and of fluctuations of times to fire as functions of the loading voltage of the (bias) electrode for several values of the loading voltage on the main electrode. Figure 7a shows the measurement system.

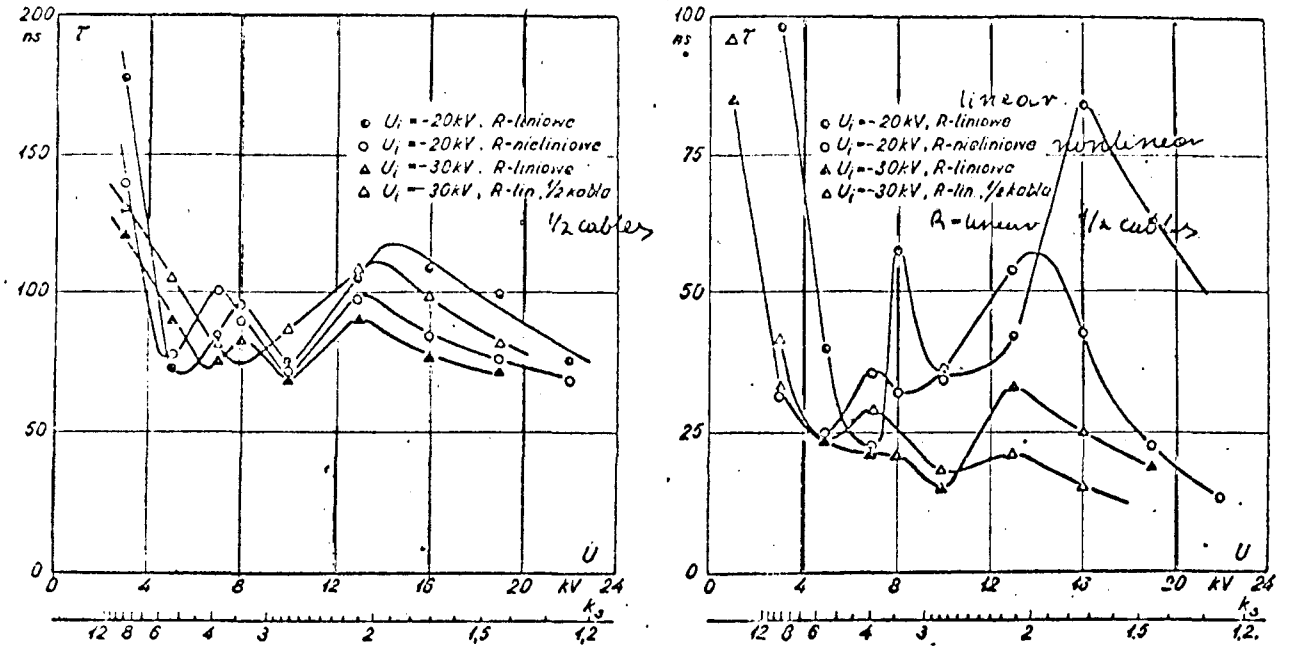

Figure 11 : Characteristics of times to fire and of fluctuations of times to fire as functions of the loading voltage on the main electrode for several values of the loading voltage on the (bias) electrode. Figure 7b shows the measurement system. (The amplitude of the loading voltage on the main electrode is additive) or (There are other changes in the value of the loading voltage on the main electrode).

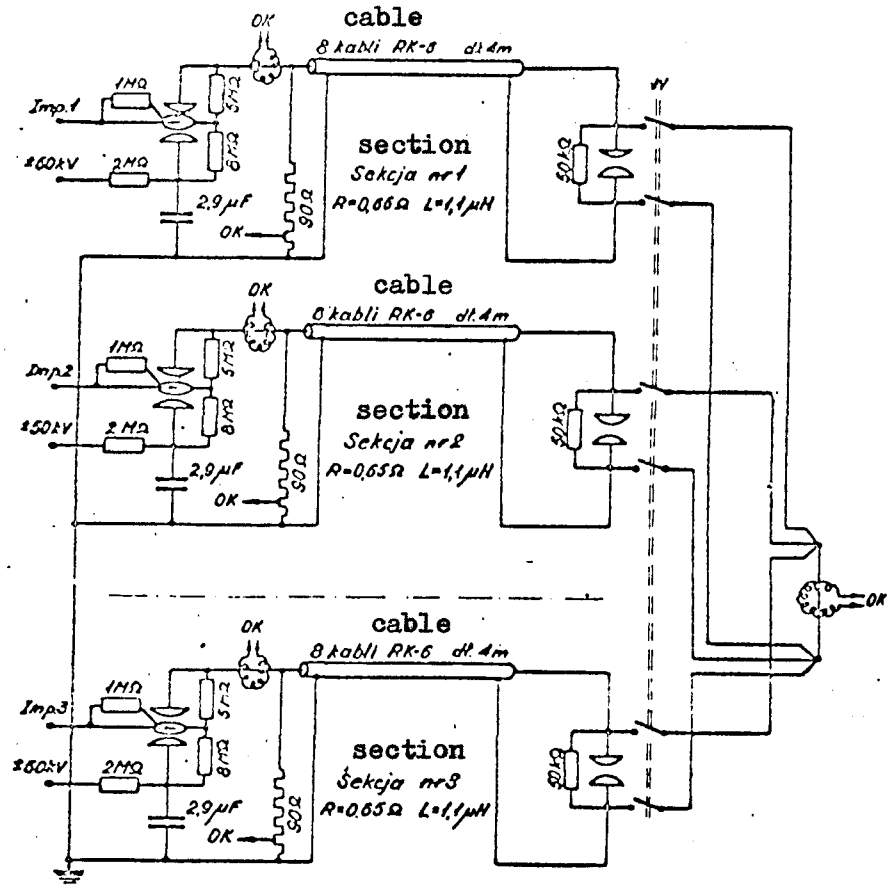

Figure 12 : Schematic representation of the impulse current generator, which was used to test the interaction of parallel spark gaps.

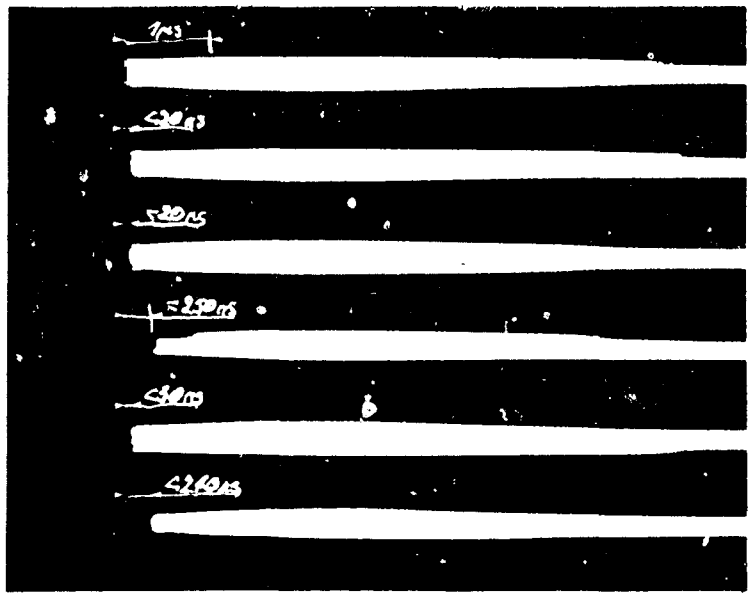

Figure 13a : A typical shadow photograph of the discharges of 6 secondary spark gaps in the configuration drawn in figure 12, using open switches. The initiating circuit is shown in figure 3a, and Ks = 2,5.

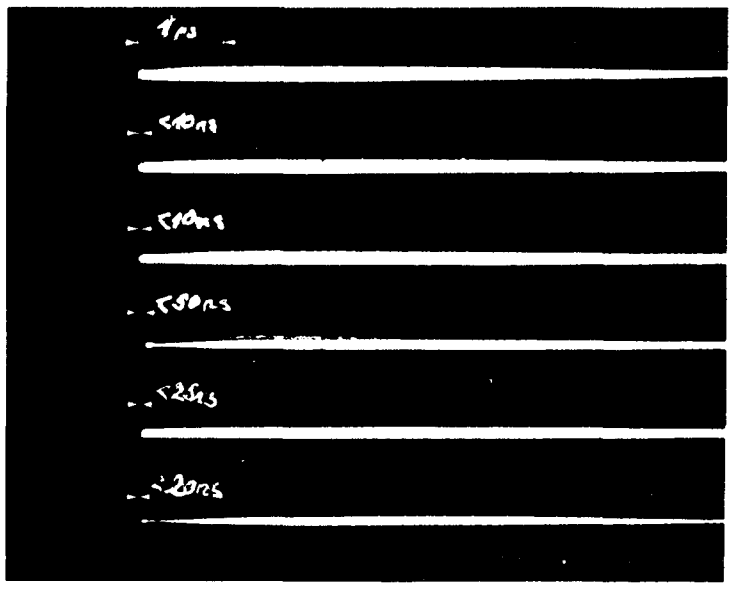

Figure 13b : A typical shadow photograph of the discharges of 6 secondary spark gaps in the configuration drawn in figure 12, using open switches. The initiating circuit is shown in figure 3b, and Ui = 30 kV, Ks = 2,1.

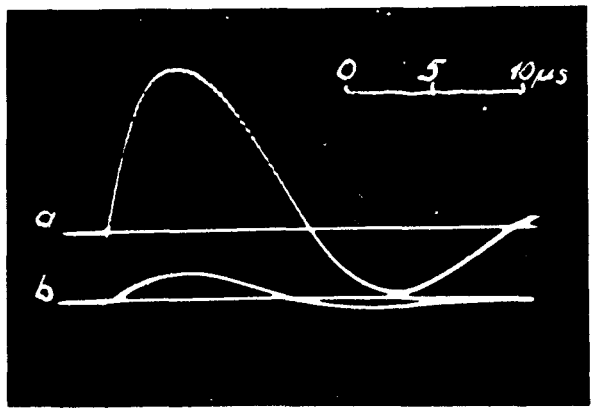

Figure 14 : Comparison of current curves :

a- total current for equal loading of the 6 sections of the generator, maximal value 73 kA.

b- current in the section 1, maximal value 12,1 kA.